

An example of the complementarity of laser-induced breakdown spectroscopy and Raman microscopy for wall painting pigments analysis

Romain Bruder,^{1,2} Vincent Detalle^{2*} and Claude Coupry³

¹ DEN/DPC/SCP/LRSI, CEA Saclay 91191 Gif sur Yvette, France

² LRMH, 29 rue de Paris 77420 Champs sur Marne, France

³ LADIR, 2 rue H. Dunant 94320 Thiais, France

Received 15 June 2006; Accepted 24 November 2006

Laser-induced breakdown spectroscopy (LIBS) and Raman microscopy were used for the identification of pigments in wall painting. Raman spectroscopy, which provides the molecular 'fingerprint' of the compound, is nowadays widely used by the archaeometry community, especially for pigment analysis. LIBS, which provides the elementary composition of samples, is a rapid noncontact method, enabling layer-by-layer analysis through a precise laser ablation of the sample. This work deals with the behavior of pigments after a LIBS analysis, by trying to identify the compounds before and after the laser shot. Six commercial pigments prepared with the fresco technique were investigated: ultramarine blue, red lead, charcoal, a yellow and a red ochre, and a green earth. Raman spectra, acquired on the sample surface and in the crater induced by LIBS analysis, were compared. The results show that these pigments are well recognized after a LIBS measurement. The analysis of green earth illustrates that the combination of these two techniques gives complete information from a sample. Copyright © 2007 John Wiley & Sons, Ltd.

KEYWORDS: LIBS; Raman microscopy; pigment analysis; wall paintings; green earth

INTRODUCTION

Numerous historical monuments are decorated with wall paintings, a valuable heritage that requires constant attention to ensure its preservation. In the case of the fresco technique, the pigments are diluted in water and applied on a fresh wet layer of lime. Then, a carbonation mechanism (reaction between carbon dioxide and lime) takes place, producing calcite. The pigments are trapped in the calcite layer. Their nature provides useful information about the history of the work of art and is essential for suitable conservation and restoration. Many techniques are employed to identify pigments on various types of works of art, such as X-ray fluorescence, X-ray diffraction, scanning electron microscopy (SEM), FT-IR spectroscopy, Raman spectroscopy, laser-induced breakdown spectroscopy (LIBS) or laser-induced fluorescence (LIF).^{1–10} A number of recent studies have shown that LIBS can be an efficient technique for the rapid identification of the elemental composition of pigments in studies of painted works of art. Owing to its quasi-nondestructive and noncontact analytical abilities,

LIBS could become a promising tool for *in situ* analysis, especially for wall paintings. Raman spectroscopy, which is widely used in archaeometric studies,^{11,12} is also a very attractive method for the identification^{13,14} of pigments since it supplies their typical 'fingerprints'. These two techniques provide different but complementary information. Another interesting feature of LIBS is its ability to 'drill' the sample, since the interaction of the laser beam with matter induces ablation of the irradiated area. An in-depth analysis is therefore possible with LIBS.^{7,15–17}

The principle of LIBS^{7,18} consists in focusing a pulsed laser beam on a sample surface for a short time (from a few femtoseconds to a few nanoseconds) with high irradiance (typically, more than a few hundreds of megawatts per square centimeter, depending on the material). The matter undergoes violent heating, which leads to its vaporization. With further laser excitation, the vapor is ionized by different phenomena. A plasma (electrons, atoms and ions in a high pressure gaseous medium) is formed, in which particles are in an excited state. These particles release photons with characteristic wavelengths to regain a stable energy level. The plasma's optical emission is then analyzed with an optical spectrometer to identify the atomic elements that are present in the sample.

*Correspondence to: Vincent Detalle, LRMH, 29 rue de Paris 77420 Champs sur Marne, France. E-mail: vincent.detalle@culture.gouv.fr

Promising experiments have been carried out to illustrate the complementarity of Raman and LIBS for rapid *in situ* measurements,^{15,19,20} but very few of them focused on the combination of the two techniques at the same location on the surface of the sample,^{16,21,22} to definitely back up its feasibility. To our knowledge, the use of LIBS' drilling capabilities to enable layer-by-layer Raman analyses of pigments have not been explicitly reported yet. One study¹⁶ only mentioned a Raman spectrum acquired from the bottom of a crater to probe the base layer of an icon after a LIBS stratigraphic analysis, but the Raman identification of pigments seems to have been carried out only on several points on the surface of the work of art. In another recent publication,²² a pulsed Raman depth-profiling on a nonlayered sample of gypsum was attempted, using alternatively LIBS and Raman laser pulses with the same instrumentation. Moreover, the complementary use of these methods could overcome the potential limitations of both spectroscopies for the identification²⁰ of pigments.

This study is the first part of a global approach focused on the *in situ* LIBS analysis of wall paintings. It was meant to illustrate the efficiency of coupling Raman microscopy with LIBS for an *in situ* analysis of fresco pigments, on a single spot of the sample. To simulate real analysis conditions, representative samples were prepared using the fresco technique. First of all, it must be pointed out that the degradation or the entire removal of the pigments due to a LIBS laser shot could be a major problem for further Raman measurements. Moreover, since for *in situ* applications the LIBS technique must result in as little damage as possible, the parameters that provide maximum safety for the artwork were investigated. Several laser energies were therefore tested. Potential degradations were tested by comparing the Raman spectra acquired on the surface of the sample and at the bottom of the LIBS crater for each pigment (Fig. 1). If Raman spectroscopy can provide correct pigment recognition, it will then enable a layer-by-layer analysis using LIBS and Raman microscopy. Then, the particular issue raised by the use of a commercial pigment called *green earth* (in fact, a blend of several compounds), highlighted for the first time to our knowledge, exemplified

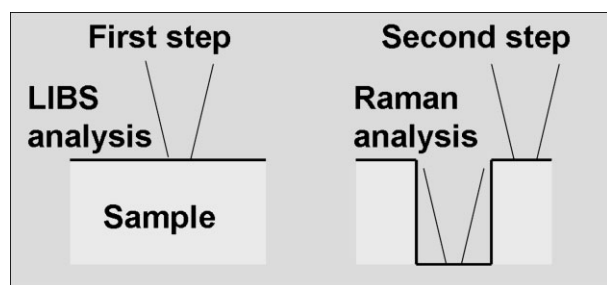


Figure 1. Principle of coupled measurement with LIBS and Raman. This figure is available in colour online at www.interscience.wiley.com/journal/jrs.

the complementarity of the two techniques, an example for which separate results are insufficient to lead to complete interpretation.

EXPERIMENTAL

LIBS instrumentation

The LIBS apparatus is represented in Fig. 2. The laser is a Minilite II Q-Switched Nd:YAG laser (Continuum, USA). The 1064 nm radiation was used for reasons of convenience: the detection system is not sensitive in the infrared domain and so is not disturbed by the diffused laser wavelength. The laser pulses had a 5 ns duration, and were triggered by the operator shot by shot. The laser energy could be set to various levels with an attenuation device integrated in the laser enclosure. The laser energy from shot to shot was controlled by a photodiode, previously calibrated with a PM500A laser power meter (Molelectron, USA) to ensure energy stability. The laser energy was successively set to four levels for each pigment: 5, 20, 35 and 50 mJ per shot, inducing four craters at different locations on the sample surface. The laser beam diameter at the focal point was about 500 μm . It was estimated by measuring the crater dimensions on a standard aluminum alloy (Péchiney Al-Mg alloy no. 970) for each energy. The laser beam, focused by a lens (100 mm focal length), struck the sample surface at normal incidence. No optimization was carried out to reduce the interaction size between the laser and the sample, and the sample position relative to the focusing lens was selected in order to provide the maximum emission signal. The emission was collected at a 45° angle with respect to the incident beam using a second lens (100 mm focal length), and was focused on a 7-fiber optical bundle (core diameter: 600 μm). Three of the fibers were connected to the entrance slits (5 μm width) of three spectrometers HR2000 (Ocean Optics, USA), which enabled the coverage of the range between 200 and 940 nm (from 200 to 340 nm, 1800 mm^{-1} grating, resolution: 0.1 nm; from

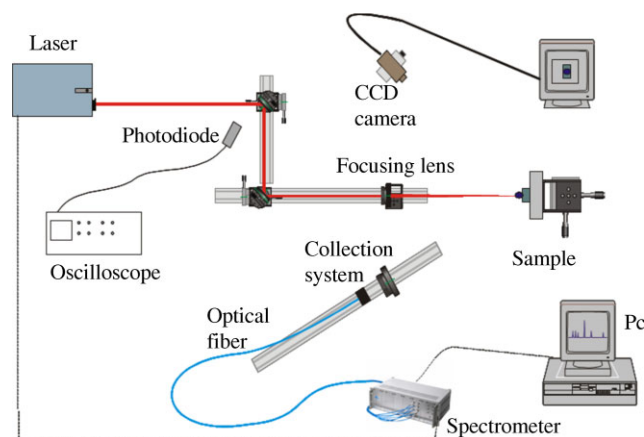


Figure 2. Experimental apparatus for LIBS analysis. This figure is available in colour online at www.interscience.wiley.com/journal/jrs.

335 to 445 nm, 1800 mm⁻¹ grating, resolution: 0.1 nm; from 510 to 940 nm, 600 mm⁻¹ grating, resolution: 0.31 nm) ensuring multielemental analysis. The emission spectrum was recorded with an internal 2048 CCD array detector (delay: 1 µs after laser Q-Switch, minimum integration time: 2.1 ms). All experiments were performed under ambient conditions.

Four energy levels were tested: for low laser energy, the molecular structure of the pigment located below the ablated volume was expected to remain unchanged. This would ensure that the Raman spectrum acquired at the bottom of the crater was mainly representative of the pigment with little contribution from the underlying mortar. If the laser energy had been set too high during a LIBS analysis, the pictorial layer could have been completely removed by a single laser shot.

Raman instrumentation

Raman microscopy measurements were performed with a LabRam microspectrometer (Horiba Jobin-Yvon). Raman excitation was obtained using the second harmonic of a CW Nd:YAG laser, at 532 nm. The use of a green laser was decided on as a compromise from the perspective of the use of a common laser source for LIBS and Raman analyses. The laser beam power was set between 0.3 and 1.4 mW on the sample surface. The laser beam diameter was 6 µm (50× magnification). Backscattered radiations were collected by the microscope and transmitted to an optical spectrometer (grating: 1800 mm⁻¹, range: 1500 cm⁻¹). The configurations for spectra acquisition typically varied from a single 30 s acquisition with a power of 0.6 mW for charcoal, to two 100 s acquisitions with a power of 0.6 mW for green earth on the surface. (The powers which were used inside the crater were: 1.4 mW for green earth, 0.6 mW for ultramarine, red lead and charcoal, and 0.3 mW for red and yellow ochres.) In particular, in the case of the analysis of the yellow and red pigments, a very low power had to be applied in order to preserve the compound's molecular structure from thermal alteration.

Samples

To simulate on-site conditions, samples were prepared with the fresco technique. The samples consisted of cellular concrete plates, covered with a first layer of mortar (coarse sand and lime). A finishing layer made of fine sand and lime was then tiered up and flattened. Pigments diluted in water were applied on this final wet coating (Fig. 3). Red lead, charcoal and ultramarine blue pigments were supplied by Kremer Pigmente, Germany, and green earth, yellow ochre and red ochre were from Ökhra, France.

The samples were preliminarily studied using a scanning electron microscope connected to an energy dispersive device for atomic identification (SEM-EDS). This examination enabled the measurement of the pictorial layer thickness on cross-sections and the identification of the elemental

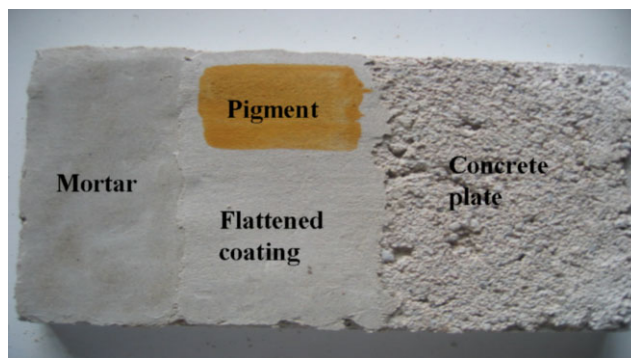


Figure 3. Composition of a sample. This figure is available in colour online at www.interscience.wiley.com/journal/jrs.

composition of the pigment, in order to later compare it with the LIBS analysis.

The thickness of the pictorial (upper) layer was measured as about 40 µm for the ultramarine blue (Fig. 4). However, many irregularities on the surface induced a thickness variation ranging from 15 to 45 µm. For the other pigments also similar observations were made, with a thickness ranging from 15 to 50 µm. EDS spectra confirmed the pictorial layer constituents for each pigment: Na, Al, Si, O and S for ultramarine blue, along with Ca, C and O, for calcite. A weak signal from elements such as Mg, K or Cl made it possible to reveal impurities (e.g. dolomite, CaMg(CO₃)₂, in calcite).

The Raman and LIBS bands obtained from the neat pigments used in this study have been summarized in Table 1. The comparison with literature data will be carried out later.

RESULTS AND DISCUSSION

The LIBS results of ultramarine blue and red lead will be presented first, to illustrate the LIBS capabilities. Craters were selected when they provided sufficient LIBS signal for the minimum laser energy, i.e. minimal effect on the sample.

For ultramarine blue, the bottom of the crater induced by a 35 mJ laser shot was mainly blue, showing the presence of the blue pigment. The different atomic constituents of the ultramarine blue (Na₈₋₁₀Al₆Si₆O₂₄S₂₋₄) were expected to be detected in the LIBS spectrum, along with calcium from calcite (fresco technique). Figure 5 presents two parts of the LIBS spectrum, from 275 to 325 nm and from 585 to 595 nm, which clearly show the characteristic emission lines of atomic elements: Na (588.99, 589.59 nm), Si (288.16 nm) and Al (308.21, 309.27 nm), and a signal due to calcium emission (315.89, 317.93 nm). Other major lines of these elements also appeared on the spectrum: 221.17 and 221.81 nm for Si, 394.40 and 396.15 nm for Al and 393.36, 396.84 and 422.67 nm for Ca. These results provided valuable information in accordance with the known elemental composition of the pigment. Impurities were present: magnesium (Mg I at 285.21 nm, Mg II at 279.55 and 280.27 nm) could be easily observed.

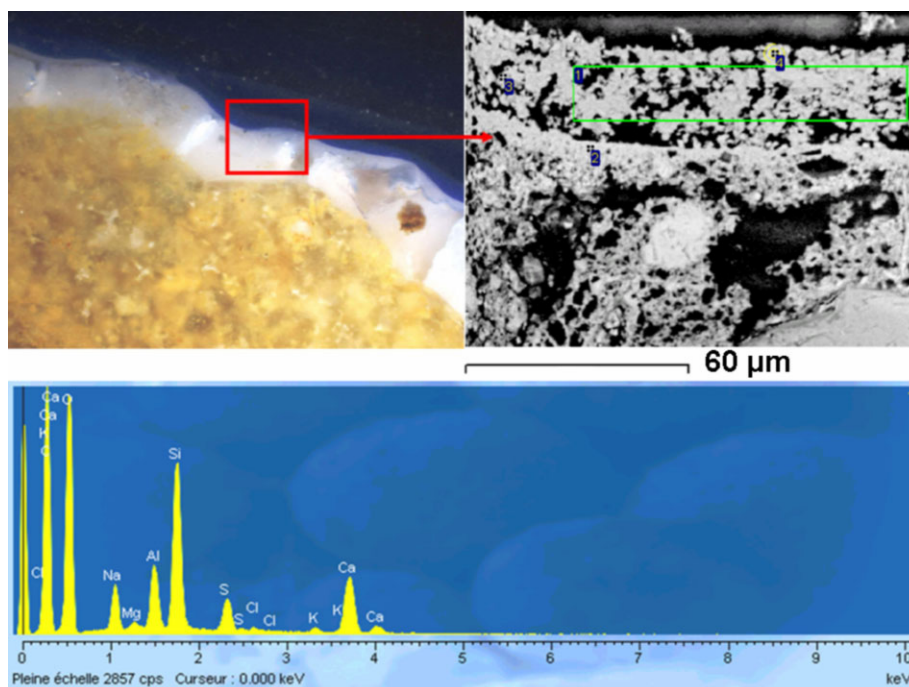


Figure 4. Optical (a) and SEM (b) images, and EDS spectrum (c) of the ultramarine blue pictorial layer. The spectrum corresponds to the mean spectrum from the zone shown by the rectangle in the SEM image. This figure is available in colour online at www.interscience.wiley.com/journal/jrs.

Table 1. Raman and LIBS bands of pigments and calcium compounds (used in this study). The symbol (II) corresponds to a line of the ionized element

Pigments	Raman shifts (cm^{-1})	Atomic elements and their LIBS emission line wavelengths (nm)
Ultramarine blue (Kremer 45010)	256, 548, 583, 806, 1096, 1357	Na 588.99/589.59; Al 308.21/309.27/394.40/396.15; Si 288.16/390.55
Red lead (Kremer 42500)	142, 228, 390, 478, 547	Pb 220.35 (II)/280.20/283.30/363.96/368.35/405.78
Brentonico green earth (Okhra)	387, 509, 685, 739, 775, 818, 960, 980, 1201, 1215, 1284, 1292, 1304, 1339, 1348, 1361, 1390, 1447, 1483, 1507, 1539, 1550, 1563	K 766.49/769.90; Al 308.21/309.27/394.4/396.15; Fe 247.29/275.01/275.73/300.1; Mg 279.55 (II)/280.27 (II)/285.21; Si 288.16/390.55
Charcoal (Kremer 47800)	1340, 1605	C 247.85
Red ochre (Okhra)	230, 298, 414, 676, 1345	Fe 238.20 (II)/248.33/382.04/404.58; Al 308.21/309.27/394.40/396.15; Si 288.16/390.55
Yellow ochre (Okhra)	400, 560, 695	Fe 238.20 (II)/248.33/382.04/404.58; Al 308.21/309.27/394.40/396.15; Si 288.16/390.55
Calcite	158, 283, 712, 1088	Ca 315.89 (II)/317.93 (II)/370.60 (II)/373.69 (II)/393.37 (II)/396.85 (II)/422.67
Gypsum	414, 495, 1007, 1137	–

The high sensitivity of these magnesium emission lines, displaying strong lines even for a concentration of only a few ppm is well known.

A single shot of 50 mJ induced a crater in the pictorial layer of red lead (minium; Pb_3O_4). The LIBS spectrum of

red lead (360–440 nm) is presented in Fig. 6. Emission peaks are easily assigned to lead (363.96, 368.35, 405.78 nm) and calcium (370.60, 373.69, 393.37, 396.85, 422.67, 430.25 nm). The LIBS (and further Raman) spectra combine those of the pigment and calcite.

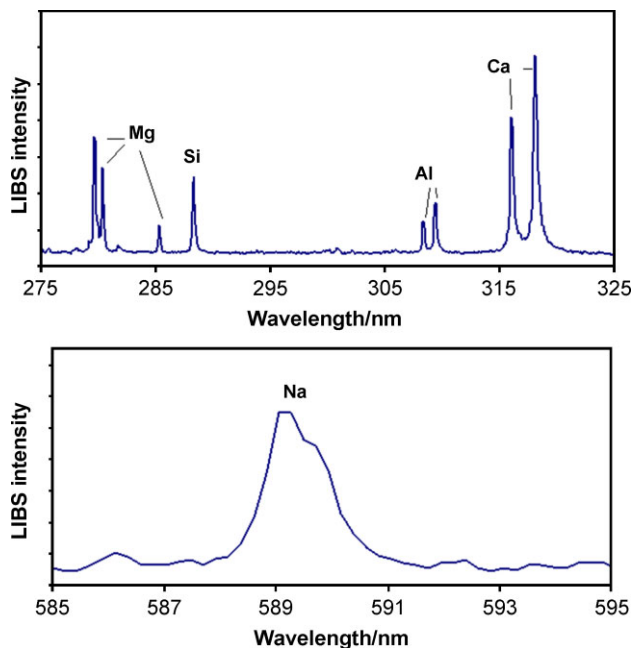


Figure 5. LIBS spectrum of the ultramarine blue sample. The spectrum was acquired for a single laser shot: laser energy, 35 mJ; exposure time, 2.1 ms. This figure is available in colour online at www.interscience.wiley.com/journal/jrs.

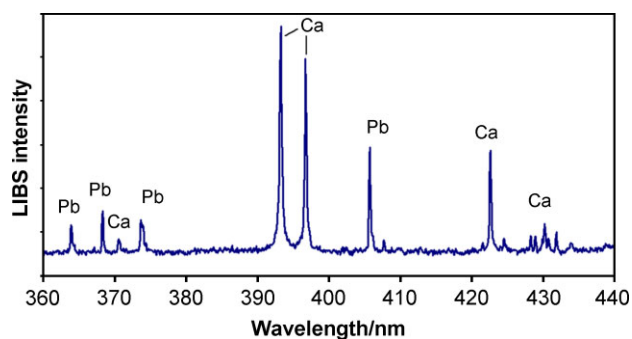


Figure 6. LIBS spectrum of red lead sample. Spectrum acquired for a single laser shot. Laser energy, 50 mJ; exposure time, 2.1 ms. This figure is available in colour online at www.interscience.wiley.com/journal/jrs.

With the selected settings, the LIBS analysis provides valuable results since the elemental composition obtained allows pigment recognition, and produces craters from the bottom of which Raman measurements can be made.

The experiments carried out consisted in comparing Raman spectra obtained on the surface and at the bottom of the crater in order to verify the presence of the characteristic Raman bands of the pigment after the LIBS analysis. The crater diameter was measured for the whole area presenting visible color attenuation under an optical microscope; owing to laser ablation, the thickness of the pigment decreased, which induced a less intense color of the sample. The laser diameter for the Raman analysis, set to 6 μm , was much

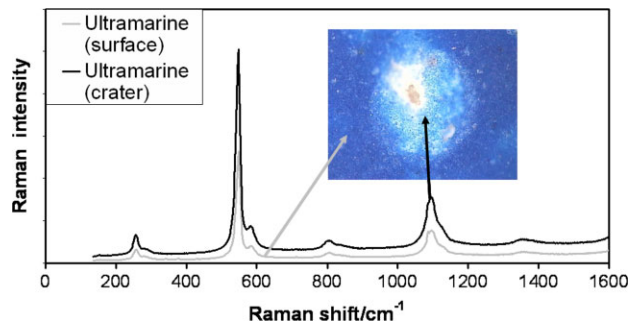


Figure 7. Raman spectra of the ultramarine blue sample and the image of the LIBS crater (inset). The crater was induced by a single laser shot of 35 mJ, diameter 440 μm . This figure is available in colour online at www.interscience.wiley.com/journal/jrs.

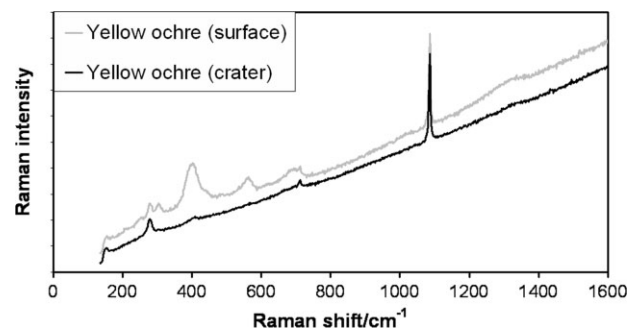


Figure 8. Raman spectra of the yellow ochre sample. The crater was induced by a single laser shot of 50 mJ, diameter 440 μm .

smaller than the crater diameter, so as to probe only the zone of interest without any surface interference. The beam was aimed at the estimated center of the crater. For ultramarine blue (Fig. 7), the selected crater was induced by a 35 mJ laser shot and presented a 440 μm diameter. The spectra both on the surface and at the bottom of the crater were in good agreement: bands at 256, 548, 583, 806, 1096 and 1357 cm^{-1} were easily identified in both cases. Raman scattering from calcite was observed with the two major peaks at 283 and 1088 cm^{-1} . Three other pigments presented the same kind of results, providing the characteristic pigment bands, combined with calcite, for both places of analysis (Table 1): red lead (crater 50 mJ, 675 μm diameter), charcoal (crater: 50 mJ, 675 μm diameter) and red ochre (crater: 50 mJ, 460 μm diameter).

In the case of yellow ochre (crater: 50 mJ, 440 μm diameter), the obtained results were not as convincing as the previous observations. Raman bands were visible for the spectrum collected on the sample surface, at 400, 560 and 695 cm^{-1} . However, only the 400 cm^{-1} broad band (goethite) could be seen in the spectrum acquired inside the crater, with a high fluorescence level (Fig. 8).

The results for ultramarine blue, red lead, charcoal and red ochre showed the feasibility of performing Raman

microscopy in a LIBS crater since it was possible to identify the specific bands assigned to the pigment on the sample surface and inside the crater. In both cases, the Raman spectra showed features due to the pigment and calcite, which means that the LIBS laser shot did not remove the whole pigment layer but preserved it sufficiently for Raman identification. A complementary stratigraphic study will be considered, with the acquisition of a Raman spectrum after each successive LIBS laser shot at the same place on the sample.

The reasons for the weakness of the yellow ochre signal were probably the Raman experimental conditions: yellow ochre is a delicate pigment, requiring very low laser powers to prevent the goethite from heating, which can transform it into hematite. The spectrum collected here showed no obvious features, highlighting the fact that no transformation into hematite could be clearly observed.

The identification of pigments using LIBS can be performed in low laser energy conditions in order to avoid the ablation of the entire thickness of the pictorial layer. Nevertheless, the preliminary SEM study indicates that without specific optimization of the LIBS system parameters (and especially laser parameters such as wavelength and beam shape), depth resolution in this study is better than 40 μm .

The specific case of green earth (Brentonico green earth from Okhra) illustrates the performance of the complementarity between the two methods. It enables overcoming the limitations of both techniques.

The LIBS spectrum (Fig. 9) of the green pictorial layer showed emission lines from atomic elements constituting this earth pigment: Al (308.21, 309.27, 394.4, 396.15 nm), Si (288.16, 390.55 nm), Fe (238.2, 248.33, 382.04, 404.58 nm), K (766.49, 769.9 nm) and Mg (279.55, 280.27, 285.21 nm). The Raman spectra (Fig. 10) were similar, with different intensities outside and inside the crater (crater: 50 mJ, 460 μm diameter). After the elimination of some bands assigned to calcite (158, 283, 712 and 1088 cm^{-1}) and gypsum (414, 495, 1007 and 1137 cm^{-1}), the bands at 509, 642, 685, 739, 775, 818, 980, 1201, 1215, 1284, 1292 (sh), 1304, 1339, 1361, 1390, 1447, 1483, 1507, 1539, 1550(sh) and 1563 cm^{-1} were not in agreement with those expected for an aluminosilicate like green earth. The reference spectra were obtained for the mineralogical compound from samples of two types of green earth provided by the *Museum National d'Histoire Naturelle* (Paris, France) and published for one.²³ This was in accordance with the literature^{24,25} or data from studies on wall paintings.²⁶ On the contrary, this spectrum is similar to that of a contemporary green pigment, phthalocyanin green.²⁷ A new LIBS analysis (Fig. 11) was performed on the commercial green earth used in this study which made it possible to detect a low quantity of copper, along with titanium (the presence of 1.44% TiO_2 was confirmed by the supplier). Thus, Raman data allowed only the observation of phthalocyanin green without indicating that green earth was really present in this pigment. This did not correspond to the results obtained by LIBS analysis, which revealed

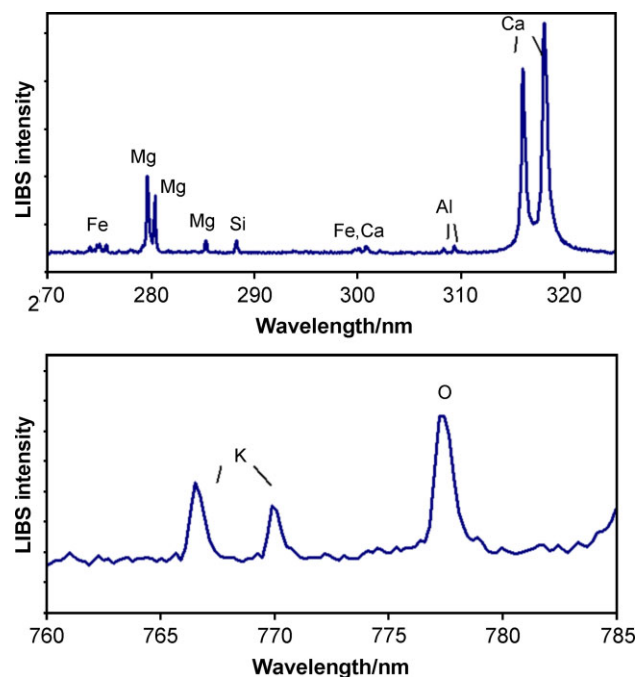


Figure 9. LIBS spectrum of green earth sample. The spectrum was acquired for a single laser shot. Laser energy, 50 mJ; exposure time, 2.1 ms. This figure is available in colour online at www.interscience.wiley.com/journal/jrs.

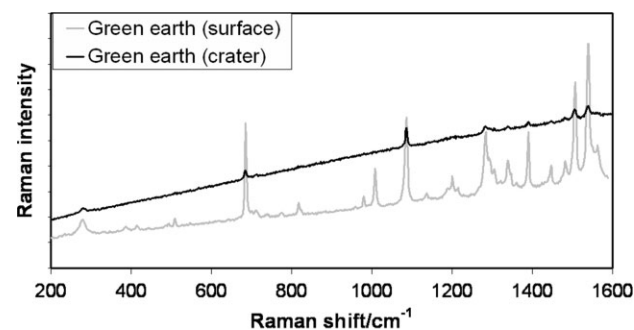


Figure 10. Raman spectra of green earth sample. The crater was induced by a single laser shot of 50 mJ, diameter 460 μm .

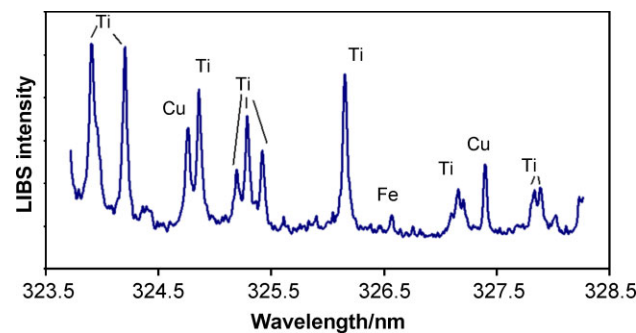


Figure 11. LIBS spectrum of the green earth sample with focus on copper. The spectrum was acquired for 10 laser shots. Laser energy, 35 mJ; exposure time per shot, 2 μs . This figure is available in colour online at www.interscience.wiley.com/journal/jrs.

the characteristic elements of green earth. In the end, the Italian supplier confirmed that this pigment was green earth, mixed with phthalocyanin green (0.3%) to give the pigment a deeper hue. The case reported here shows that LIBS or Raman analysis alone sometimes cannot provide the complete information and may lead to an incomplete interpretation. However, their combination makes it possible to overcome the limitations of both techniques. It also points out the difficulty in obtaining reliable information from contemporary pigments for the study of ancient paintings. Some green earth reference spectra in the literature showed strong similarities with the spectrum of phthalocyanin green and could be suspected to have been obtained with a blend of a similar pigment. In this mixture, green earth + phthalocyanin green, LIBS analysis did not easily detect copper present in very small quantities, while Raman analysis did not detect green earth, the intensity of which is very low in contrast to phthalocyanin.

CONCLUSIONS

This study confirms the efficiency of using such a combination of techniques in pigment identification. From this example, a procedure for pigment identification could be proposed. From a database containing the chemical formula and the color of known pigments, an adapted LIBS system would be able to identify the presence or absence of characteristic atomic emission lines to give a first estimation of the nature of the pigment. The molecular nature of the pigment can then be obtained by Raman analysis. However, in the case of a combination of pigments, the interpretation becomes more complex. When the relative sensitivities or the relative concentration of the components are very different, or when the same atomic elements are present in each pigment in the mixture, LIBS or Raman spectrometry cannot be accurate enough to clearly identify the pigments. A combination with other techniques would then be necessary. The major result of this study is that Raman spectroscopy can be used after a single-shot LIBS analysis inside the crater to identify the molecular nature of the pigments and to confirm or complete the hypothesis suggested by the LIBS measurement. It must be noted that LIBS can also help Raman spectrum interpretation, as shown by the case of green earth in this study. Further studies will be carried out to improve the LIBS settings, in order to find better in-depth resolution with maximum signal for LIBS analysis. A further study will especially focus on the choice of the laser wavelength. Regarding the laser effect for both techniques, it is worth noting that for this study the hardest conditions in Raman (1.4 mW during 60 s with a 6- μm laser beam diameter) represent an irradiance of $4.95 \times 10^3 \text{ W cm}^{-2}$ and a fluence of $2.97 \times 10^5 \text{ J cm}^{-2}$, whereas the hardest conditions in LIBS (50 mJ with 5 ns pulse duration and 500 μm laser beam

diameter) correspond to an irradiance of $5.1 \times 10^9 \text{ W cm}^{-2}$ and a fluence of $2.55 \times 10^1 \text{ J cm}^{-2}$. LIBS induces strong and rapid heating of the surface, localized in a small volume, which mainly leads to a mechanical effect (ablation), while the Raman technique may induce longer and gradual heating, which can essentially provoke a thermal effect on the sample.

REFERENCES

- Gilbert B, Denoël S, Weber G, Allart D. *Analyst* 2003; **128**: 1213.
- Castillejo M, Martín M, Oujja M, Rebollar E, Domingo C, García-Ramos JV, Sánchez-Cortés S. *J. Cult. Herit.* 2003; **4**: 243.
- Anglos D, Balas C, Fotakis C. *Am. Lab.* 1999; **31**: 60.
- Weis TL, Jiang Y, Grant ER. *J. Raman Spectrosc.* 2004; **35**: 813.
- Borgia I, Burgio L, Corsi M, Fantoni R, Palleschi V, Salvetti A, Squarcialupi MC, Tognoni E. *J. Cult. Herit.* 2000; **1**(Suppl. 1): 281.
- Perardi A, Zoppi A, Castellucci E. *J. Cult. Herit.* 2000; **1**(Suppl. 1): 269.
- Anglos D, Couris S, Fotakis C. *Appl. Spectrosc.* 1997; **51**: 1025.
- Vandenabeele P, Wehling B, Moens L, Edwards H, De Reu M, Van Hooydonk G. *Anal. Chim. Acta* 2000; **407**: 261.
- Hochleitner B, Desnica V, Mantler M, Schreiner M. *Spectrochim. Acta, Part B* 2003; **58**: 641.
- Castillejo M, Martín M, Oujja M, Silva D, Torres R, Domingo C, García-Ramos JV, Sánchez-Cortés S. *Appl. Spectrosc.* 2001; **55**: 992.
- Smith GD, Clark RJH. *J. Arch. Sci.* 2004; **31**: 1137.
- Smith GD, Clark RJH. *Rev. Conserv.* 2001; **2**: 92.
- Bell IM, Clark RJH, Gibbs PJ. *Spectrochim. Acta, Part A* 1997; **53**: 2159.
- Burgio L, Clark RJH. *Spectrochim. Acta, Part A* 2001; **57**: 1491.
- Castillejo M, Martín M, Silva D, Stratoudaki T, Anglos D, Burgio L, Clark RJH. *J. Mol. Struct.* 2000; **550–551**: 191.
- Burgio L, Clark RJH, Stratoudaki T, Doulgeridis M, Anglos D. *Appl. Spectrosc.* 2000; **54**: 463.
- Golovlev VV, Gresalfi MJ, Miller JC, Anglos D, Melessanaki K, Zafropoulos V, Romer G, Messier P. *J. Cult. Herit.* 2003; **4**(Suppl. 1): 134.
- Radziemski LJ, Cremers DA. *Laser-induced Plasmas and Applications*. Marcel Dekker, Inc.: New York, Basel, 1989; 295.
- Bicchieri M, Nardone M, Russo PA, Sodo A, Corsi M, Cristoforetti G, Palleschi V, Salvetti A, Tognoni E. *Spectrochim. Acta, Part B* 2001; **56**: 915.
- Burgio L, Melessanaki K, Doulgeridis M, Clark RJH, Anglos D. *Spectrochim. Acta, Part B* 2001; **56**: 905.
- Marquardt BJ, Stratis DN, Cremers DA, Angel SM. *Appl. Spectrosc.* 1998; **52**: 1148.
- Giakoumaki A, Osticioli I, Anglos D. *Appl. Phys. A* 2006; **83**: 537.
- Coupry C, Lautié A, Sagon G, Froment F. In *Raman Spectroscopy in Archaeology and Art History*, Edwards HGM, Chalmers JM (eds). Royal Society of Chemistry: London, 2005; 207.
- Daniilia S, Bikiaris D, Burgio L, Gavala P, Clark RJH, Chryssoulakis Y. *J. Raman Spectrosc.* 2002; **33**: 807.
- Villar SEJ, Edwards HGM. *Anal. Bioanal. Chem.* 2005; **382**: 283.
- Middleton PS, Ospitali F, di Leonardo G. In *Raman Spectroscopy in Archaeology and Art History*, Edwards HGM, Chalmers JM (eds). Royal Society of Chemistry: London, 2005; 97.
- Barbet A, Coupry C, Lautié A. In *Proceedings of the International Workshop "Roman Wall painting, Materials, Analysis, and Conservation"*, Fribourg, CH, 1997; 257.